A Combined Raman and Deuterium NMR Spectroscopic Study on the Molecular and Phase Structure of a Nonionic Surfactant $C_{12}E_5$−Water System

Akimitsu Tonegawa, Keiichi Ohno,* Hiroatsu Matsuura, Koji Yamada, and Tsutomu Okuda

Department of Chemistry, Graduate School of Science, Hiroshima University, Kagamiyama, Higashi-Hiroshima 739-8526, Japan

Received: July 31, 2002; In Final Form: October 3, 2002

A combined C−D stretching Raman and deuterium NMR spectroscopic method was applied to a study of the molecular and phase structure of the $C_{12}E_5$−water system, where $C_{12}E_5$ denotes a nonionic surfactant $CH_3(CH_2)_{11}(OCH_2CH_2)_5OH$. Spectroscopic measurements were performed on aqueous solutions of six selectively alkyl-monodeuterated species, an oxyethylene-partially deuterated species, an alkyl-*block*-deuterated species, and an oxyethylene-*block*-deuterated species. The ranges of the compositions and temperatures studied were 40−75 wt % $C_{12}E_5$ and 0−80 °C, where a number of anisotropic and isotropic phases are observed. The Raman results showed that the trans fractions of the C−C bonds of the dodecyl chain decrease continuously with increasing temperature across different phases. The NMR results showed, on the other hand, that, with increasing temperature, the order parameters exhibit distinct discontinuities at the phase transition from the normal hexagonal phase to the lamellar phase. The results from the two spectroscopic methods reflect the difference in their time scale. The behavior of the order parameters was explained by taking account of two factors, the chain order and the conformational order. The observed discontinuities of the order parameters at the phase transition can be ascribed to the change of the chain order, which is caused by wobbling motions of the whole surfactant molecule. The temperature-dependent shift of the position on the alkyl chain, at which the order parameters show their maximum, is explained by the different rates of reduction, with increasing temperature, of van der Waals forces between the alkyl chains and hydrogen-bonding forces between the oligo(oxyethylene) chain and water. The stability of the lamellar phase is maintained by the presence of interlamellar water.

Introduction

Amphiphilic molecules composed of hydrophilic and hydrophobic moieties aggregate in solvents to form a variety of supramolecular structures, most of which yield lyotropic liquid-crystalline phases.[1−5] In fact, systems of surfactants and water exhibit interesting phase behavior with varying composition and temperature.[6−10] Most commonly encountered liquid-crystalline phases are lamellar, hexagonal (normal and reversed), and cubic (normal and reversed), which have been well characterized by various experimental techniques. The phase behavior is correlated to an effective cross-sectional area of the hydrophobic/hydrophilic interface per amphiphilic molecule and an effective length of the hydrophobic and/or hydrophilic chain in liquid-crystalline phases.[5,8] These geometrical properties in turn result from the conformation of the molecule. Thus, the conformational state of the molecule as well as the chain order in liquid-crystalline phases is an important subject to study for elucidating the mechanism of phase behavior.

The conformation of surfactant molecules in the aggregated structures has been studied in most cases by vibrational spectroscopy, that is, infrared spectroscopy and Raman spectroscopy, since the properties of molecular vibrations, in particular the wavenumbers[11,12] of vibrations, are highly sensitive to the conformational state of the molecule.[13,14] Actually, in a series of Raman studies of melting transitions of phospholipids, Peticolas et al. have discussed conformations of alkyl chains using C−H and C−D stretching vibrations.[15−19] In our previous work,[20−25] we have proposed and utilized a method of analyzing wavenumbers of isolated C−D stretching vibrations to determine the conformation of a specified site of the molecular chain. Using a number of monodeuterated species in which one of the hydrogen atoms at different positions in the chain is selectively substituted by deuterium, we can eventually determine the conformational state of the whole chain.

For studying the order of molecular chains in liquid-crystalline phases, deuterium NMR spectroscopy is one of the powerful experimental techniques.[26−29] With this technique, information of motionally averaged C−D bond orientation is obtained through the quadrupole interaction of the deuterium nucleus with the electric field gradient. We have applied this method to studies of the structure of liquid-crystalline phases that contain a nonionic surfactant.[30−32]

We propose to combine the two spectroscopies, vibrational spectroscopy and deuterium NMR spectroscopy, to make a comprehensive study of the structure of liquid crystals. An essential advantage of this combination is that the two spectroscopies are complementary in that, while vibrational spectroscopy (infrared and Raman) observes molecular motions on a time scale of 10^{-14} to 10^{-13} s, NMR spectroscopy observes those on a time scale of 10^{-5} to 10^{-4} s. In NMR experiments, if the molecular motion is of the order of 10^{-15} to 10^{-6} s, then the nuclear spins experience motionally averaged spin interactions.[33] The relevant motions are internal molecular motions such as conformational changes, molecular rotations such as

* To whom correspondence should be addressed. E-mail: kohno@sci.hiroshima-u.ac.jp.

10.1021/jp021760u CCC: $22.00
Published on Web 12/03/2002

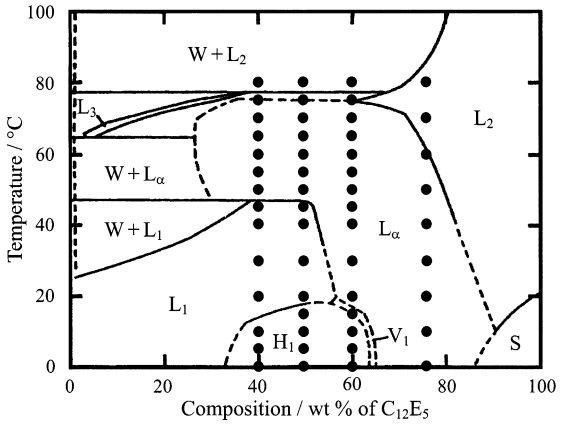

Figure 1. Phase diagram of the $C_{12}E_5$−water system.[8] The temperatures and compositions at which the spectral measurements were performed are indicated by dots.

molecular orientations, and molecular translations. Using the two spectroscopic techniques, we can study simultaneously conformational changes (10^{-11} to 10^{-10} s) of the molecule (vibrational spectroscopy) and the motionally averaged orientation of the chain (NMR spectroscopy), and can elucidate eventually the overall dynamical structural properties of the molecular systems of liquid crystals.

In our previous work,[22,23,25] we have studied the conformational behavior of a nonionic surfactant, $CH_3(CH_2)_{11}(OCH_2CH_2)_3OH$ (abbreviated as $C_{12}E_3$), in a binary system with water using C−D stretching infrared spectroscopy. The same binary system was also investigated by deuterium NMR spectroscopy.[30] The NMR spectroscopic method was further applied to a ternary system, $C_{12}E_3$−decane−water.[31] This ternary system was subsequently examined by combined use of the Raman and deuterium NMR spectroscopic methods.[32] In light of the results of these preceding studies, we have performed in this work a combined Raman and deuterium NMR spectroscopic study on the molecular and phase structure of the $C_{12}E_5$−water system in relation to its phase behavior, where $C_{12}E_5$ denotes $CH_3(CH_2)_{11}(OCH_2CH_2)_5OH$ (α-dodecyl-ω-hydroxypentakis(oxyethylene)). The phase diagram of the $C_{12}E_5$−water system has been reported by Mitchell et al.[8] and is cited in Figure 1.

In this work, we employed the following nine deuterated species of $C_{12}E_5$: $CH_3(CH_2)_{10}CHD(OCH_2CH_2)_5OH$ (C_{12}-1-d_1-E_5), $CH_3(CH_2)_9CHDCH_2(OCH_2CH_2)_5OH$ (C_{12}-2-d_1-E_5), $CH_3(CH_2)_7CHD(CH_2)_3(OCH_2CH_2)_5OH$ (C_{12}-4-d_1-E_5), $CH_3(CH_2)_5CHD(CH_2)_5(OCH_2CH_2)_5OH$ (C_{12}-6-d_1-E_5), $CH_3(CH_2)_3CHD(CH_2)_7(OCH_2CH_2)_5OH$ (C_{12}-8-d_1-E_5), $CH_3CH_2CHD(CH_2)_9(OCH_2CH_2)_5OH$ (C_{12}-10-d_1-E_5), $CD_3(CD_2)_{10}CH_2(OCH_2CH_2)_5OH$ (C_{12}-d_{23}-E_5), $CH_3(CH_2)_{11}(OCD_2CD_2)_5OH$ ($C_{12}E_5$-d_{20}), and $CH_3(CH_2)_{11}(OCD_2CD_2)_3(OCH_2CH_2)_2OH$ ($C_{12}E_3$-d_{12}-E_2). The carbon atoms in the $C_{12}E_5$ molecule are numbered as $HO-C_{10'}-C_{9'}-O-\cdots-O-C_{4'}-C_{3'}-O-C_{2'}-C_{1'}-O-C_1-C_2-\cdots-C_{11}-C_{12}$.

Experimental Section

Materials. Six selectively alkyl-monodeuterated species of $C_{12}E_5$, namely C_{12}-1-d_1-E_5, C_{12}-2-d_1-E_5, C_{12}-4-d_1-E_5, C_{12}-6-d_1-E_5, C_{12}-8-d_1-E_5, and C_{12}-10-d_1-E_5, and an oxyethylene-partially deuterated species, $C_{12}E_3$-d_{12}-E_2, were prepared by the reaction of *p*-toluenesulfonates of the corresponding species of $C_{12}E_3$ with diethylene glycol following a procedure similar to that of Sekera and Marvel.[34] The syntheses of the precursor $C_{12}E_3$ species were reported previously.[23,35,36] The alkyl-*block*-deuterated species C_{12}-d_{23}-E_5 and the oxyethylene-*block*-deuterated species $C_{12}E_5$-d_{20} were synthesized from the pertinent 1-chlorododecane and pentaethylene glycol by the Williamson method. Perdeuterated 1-chlorododecane and perdeuterated pentaethylene glycol were prepared by an H/D exchange reaction with D_2O in the presence of a Pd-catalyst in a small autoclave maintained at about 200 °C.[37,38] The products were purified by column chromatography and subsequently by vacuum distillation. The purity of the products was checked by gas chromatography to be better than 97%.

Raman and Infrared Measurements. Raman spectra were measured on a JASCO NR-1800 spectrometer equipped with a Princeton Instruments CCD detector with a spectral resolution of 3 cm^{-1}. An NEC argon ion laser GLG 2162 operating at 514.5 nm was used for excitation. Raman spectra of aqueous solutions of C_{12}-1-d_1-E_5, C_{12}-2-d_1-E_5, C_{12}-4-d_1-E_5, C_{12}-6-d_1-E_5, C_{12}-8-d_1-E_5, and C_{12}-10-d_1-E_5 were measured at four compositions, 40, 50, 60, and 75 wt % $C_{12}E_5$, in the temperature range from 0 to 80 °C. The temperatures and compositions at which the spectral measurements were performed are indicated by dots in Figure 1. The temperature of the sample contained in a sealed glass ampule was held constant during the measurement within ±0.2 °C in the 0−30 °C range by an Oxford Instruments Optistat cryostat and within ±1 °C in the 35−80 °C range by a homemade thermostat. The background of the spectra was corrected by subtracting the Raman spectrum of the undeuterated species of $C_{12}E_5$ from that of the monodeuterated species of $C_{12}E_5$ in question at the same composition and temperature. Special care was taken in measuring the Raman spectra of the isotropic and anisotropic phases, since these phases have different polarization properties, as will be discussed later. The observed spectral profiles of the C−D stretching bands were analyzed by fitting with mixed 85% Lorentzian and 15% Gaussian components using a curve-fitting subroutine of the GRAMS/32 software package (Galactic Industries, Salem, NH).

The infrared spectra of aqueous solutions of $C_{12}E_5$ were measured in transmission geometry on a Bruker IFS66V spectrometer equipped with a deuterated triglycine sulfate (DTGS) detector. The solution sample was held between two KRS-5 plates with a lead spacer of 0.1 mm thickness. The spectral resolution was 2 cm^{-1}.

Deuterium NMR Measurements. Deuterium NMR measurements were performed at a deuterium resonance frequency of 41.6375 MHz on a Matec pulsed spectrometer equipped with a homemade sample probe and a temperature controller. The NMR spectra of C_{12}-1-d_1-E_5, C_{12}-2-d_1-E_5, C_{12}-4-d_1-E_5, C_{12}-6-d_1-E_5, C_{12}-d_{23}-E_5, and $C_{12}E_5$-d_{20} were measured at the same compositions and temperatures as those for the Raman measurements. The spectra of $C_{12}E_3$-d_{12}-E_2 were measured for a 50 wt % solution at 0, 15, and 60 °C and for a 60 wt % solution at 0, 25, and 40 °C for the purpose of assigning the spectra, as will be described later. The spectra were obtained by a Fourier transformation of the free induction decay. The $\pi/2$ pulse width was 3−4 μs.

Calculations

Calculations by density functional theory were carried out with the GAUSSIAN 98 program[39] on a Linux-based personal computer (1.7 GHz Intel Pentium 4 processor). The optimized structures, wavenumbers of vibrations, Raman scattering activities, and other relevant data for pertinent conformers of the model compounds for $C_{12}E_5$, namely hexyl methyl ether and heptane, were calculated at the B3LYP/6-311+G(d,p) level (Becke's three-parameter hybrid functional[40] combined with the Lee−Yang−Parr correlation functional[41] using the 6-311+G(d,p) basis set).

Results and Discussion

Depolarization Problems in Raman Measurements. The $C_{12}E_5$−water system exhibits various phases such as lamellar (L_α), normal hexagonal (H_1), normal bicontinuous cubic (V_1), micellar solution (L_1), and reversed micellar solution (L_2) phases,[8] as shown in Figure 1. While the L_1, L_2, and V_1 phases are isotropic, the L_α and H_1 phases are anisotropic, consisting of numerous randomly oriented microscopic domains of liquid crystals. Since the isotropic and anisotropic phases have different polarization properties, special attention should be paid to the polarization problem in Raman scattering.[42,43]

In the anisotropic liquid-crystalline phases, a light beam is split into ordinary and extraordinary beams with orthogonal polarization orientations at each interface between two neighboring monodomains of liquid crystals. Thus, when the number of the domains, which the beam is intersecting, is large enough, the exciting laser beam is completely depolarized and the scattered Raman spectrum is that of randomly oriented molecules illuminated with naturally polarized light. If the intensities of the scattered light components with polarization parallel and perpendicular to that of the exciting light are given by $I_{\parallel}$ and $I_{\perp}$, respectively, then the intensities of the Raman signal components with polarization parallel and perpendicular to the direction of propagation of the exciting light are proportional to $2I_{\perp}$ and $I_{\parallel} + I_{\perp}$, respectively. As the total Raman signal polarization is scrambled, the intensity of the observed spectrum, I, is given by[42]

$$I = I_{\parallel} + 3I_{\perp} \tag{1}$$

To compare correctly the Raman spectra of the anisotropic phase with the spectra of the isotropic phase, we must have the latter spectra with their intensities proportional to $I_{\parallel} + 3I_{\perp}$. Such spectra are obtained by recording the Raman scattered light from the isotropic phase with polarization rotated to 60° with respect to the polarization of the exciting light:[42,43]

$$I_{60°} = [\cos^2(60°)]I_{\parallel} + [\sin^2(60°)]I_{\perp} = {}^1/_4 I_{\parallel} + {}^3/_4 I_{\perp} \tag{2}$$

In our experiments, we actually recorded the parallel and perpendicular Raman spectra and calculated their linear combination according to eq 2, instead of directly recording the spectra at 60° polarization. This procedure minimizes possible errors due to the uncertainty in tuning the angle of the polarization rotator.[43]

Another requirement for this scheme to give correct results is to get complete depolarization of the exciting laser beam and Raman signal for the anisotropic phases. To do this, we used scramblers made of the hexagonal phase of the Triton X 100−water system (50 wt %)[44] held between two glass plates with a Teflon spacer of 1 mm thickness. The scramblers were rapidly cooled to 0 °C to get randomly oriented microscopic domains of liquid crystals. The performance of the scramblers was tested in measurements of liquid carbon tetrachloride.

Conformational Analysis of the Alkyl Chain Using Isolated C−D Stretching Vibrations. Our previous studies[20,21] have shown that the wavenumbers of isolated C−D stretching vibrations of selectively monodeuterated alkyl chains depend on the conformation around the C−C bonds in the vicinity of the C−D bond. This conformational dependence of the C−D stretching wavenumbers is correlated directly to the lengths of the C−D bonds and their force constants.[23,24] The isolated C−D stretching vibrations can therefore be used to determine the local conformation of the C−C bonds in alkyl chains, supplemented by the data afforded by quantum chemical calculations.

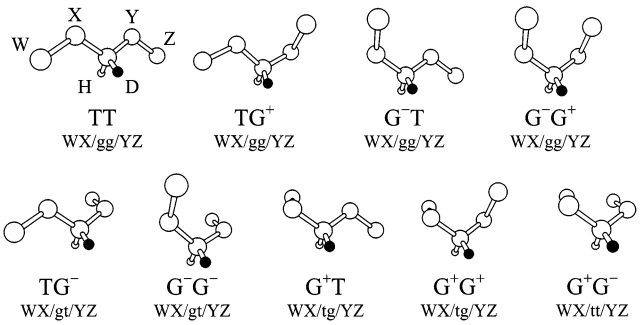

Figure 2. Molecular models of all possible conformations of a W−X−CHD−Y−Z structure with the *R*-configuration. The ascending sequence of the chemical groups H < D < Y < X has been applied. Deuterium atoms are represented by black balls.

In this work, the relevant data of structural and spectroscopic properties were obtained by performing density functional calculations at the B3LYP/6-311+G(d,p) level on hexyl methyl ether and heptane as model compounds for $C_{12}E_5$.[45] In Table 1, the calculated results of the C−D bond lengths and the diagonal force constants, Raman scattering activities, and wavenumbers of the C−D stretching vibrations for the relevant conformations of the model compounds are given together with their observed wavenumbers.[23,24]

Figure 2 shows the molecular models of all possible conformations of a W−X−CHD−Y−Z structure with the *R*-configuration, where the ascending sequence of the chemical groups H < D < Y < X has been applied. The relation between the configurations and conformations of monodeutrated compounds has been explained in our previous paper.[23] In the following, the relevant important points are cited from that paper.[23] The molecular skeletal conformations are denoted by T for trans, G^+ for gauche$^+$, and G^- for gauche$^-$ for each of the relevant single bonds. The *R*- and *S*-configurations are the enantiomers of each other and are accordingly spectroscopically equivalent in that they give the same wavenumbers of vibrations. The G^+ and G^- conformations of the *R*-configuration are spectroscopically equivalent to G^- and G^+, respectively, of the *S*-configuration. It is important to note that the methods of chemical syntheses utilized in this work yield the monodeutrated compounds with the *R*- and *S*-configurations in equal amounts.

In accordance with the notation we proposed previously,[23] the local conformation of the C−D bond in the W−X−CHD−Y−Z structure is given, for example, as WX/gt/YZ, which means that the conformation of the W−X−C−D disposition is gauche$^+$ or gauche$^-$ (g) and the conformation of the D−C−Y−Z disposition is trans (t). Using this notation, we have four types of local conformations in the vicinity of the C−D bond: WX/tt/YZ, WX/tg/YZ, WX/gt/YZ, and WX/gg/YZ. According to the data given in Table 1, the calculated C−D stretching wavenumbers for the same types of conformations are close to one another but are different from those for other types. The calculated results show the following relationship; the C−D stretching wavenumbers for the trans C−O−C−D disposition or for the trans C−C−C−D disposition are higher than those for the corresponding gauche disposition, and the C−D stretching wavenumbers for the trans O−C−C−D disposition are lower than those for the corresponding gauche disposition. The present results from the B3LYP/6-311+G(d,p) calculations are in accord with the previous results from the HF/6-31G(d,p) calculations.[23,24]

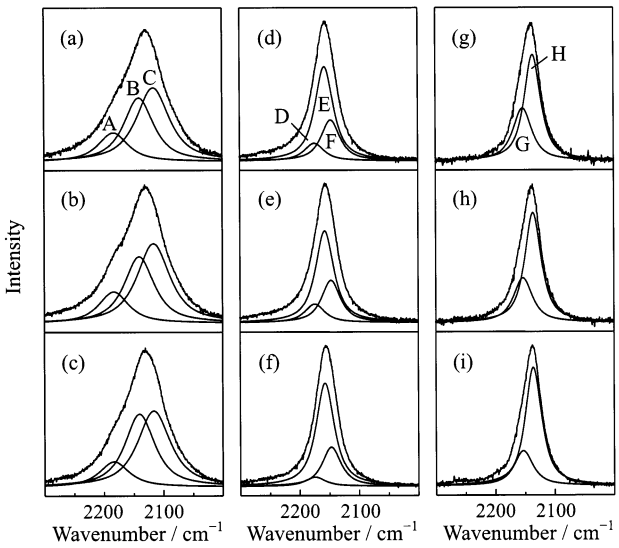

Figure 3. Raman spectra in the 2000−2300 cm^{-1} region of 50 wt % aqueous solutions of C_{12}-1-d_1-E_5 (a−c), C_{12}-2-d_1-E_5 (d−f), and C_{12}-6-d_1-E_5 (g−i) at the temperatures 70 (a, d, g), 30 (b, e, h), and 0 °C (c, f, i). Band designations (A, B, ..., H) are given in spectra a, d, and g.

Figure 3 shows typical examples of the Raman spectra in the 2000−2300 cm^{-1} region of 50 wt % aqueous solutions of C_{12}-1-d_1-E_5 (a−c), C_{12}-2-d_1-E_5 (d−f), and C_{12}-6-d_1-E_5 (g−i) at different temperatures. The observed spectral profiles of the C−D stretching vibrations are decomposed into components by fitting with the mixed 85% Lorentzian and 15% Gaussian function. The number of the components to be resolved is known beforehand from the calculated wavenumbers of the relevant model compounds (Table 1). Namely, the C−D stretching band profile for C_{12}-1-d_1-E_5 is resolved into three components (bands A, B, and C), for C_{12}-2-d_1-E_5 it is resolved into three (D, E, and F), and for C_{12}-k-d_1-E_5 (k = 4, 6, 8, and 10) it is resolved into two (G and H). Table 2 gives the parameters obtained by the band decomposition, where the wavenumbers and half widths of the respective components were assumed to be equal for all temperatures and compositions studied. The integrated areas of the resolved components were taken as their relative spectral intensities.

On the basis of the relationship between the molecular conformations and the C−D stretching wavenumbers for the model compounds (Table 1), the intensities of the respective component bands, I_A, I_B, ..., and I_H, are expressed in terms of the fractions of the pertinent conformations, f_{xy}, where x and y are either T, G^+, or G^-, for the W−X−CHD−Y−Z structure and of the Raman intensities per molecule, I_{xy}, for these conformations.[23] The intensities of bands G and H for C_{12}-k-d_1-E_5 (k = 4, 6, 8, and 10) are expressed, for example, as

$$I_G = a(f_{TG^-}I_{TG^-} + f_{G^+T}I_{G^+T} + f_{G^+G^+}I_{G^+G^+} + f_{G^-G^-}I_{G^-G^-}) \quad (3)$$

and

$$I_H = a(f_{TT}I_{TT} + f_{G^-T}I_{G^-T} + f_{TG^+}I_{TG^+}), \quad (4)$$

where a is an appropriate constant.

There are several relations of the conformation fragments f_{xy}.[23] In the case of the C−C−CHD−C−C structure, we have the following relations: $0 \le f_{TT} \le 1$, $0 \le f_{TG^+} = f_{TG^-} = f_{G^+T} = f_{G^-T} \le 0.25$, $0 \le f_{G^+G^+} = f_{G^-G^-} \le 0.5$, and $f_{TT} + 4f_{TG^+} + 2f_{G^+G^+} = 1$, where $f_{G^+G^-}$ and $f_{G^-G^+}$ have been assumed to be zero, because the G^+G^- and G^-G^+ sequences have exceedingly higher energies than other conformational sequences.[46] The trans fractions of the X−C and C−Y bonds in the W−X−CHD−Y−Z structure are given by $f_T(X-C) = f_{TT} + f_{TG^+} + f_{TG^-}$ and $f_T(C-Y) = f_{TT} + f_{G^+T} + f_{G^-T}$, respectively. The values of the conformation fragments obtained for C_{12}-k-d_1-E_5 (k = 4, 6, 8, and 10) are those averaged over the two adjacent C−C bonds, as we have assumed that $f_{TG^+} = f_{TG^-} = f_{G^+T} = f_{G^-T}$ for the C−C−CHD−C−C structure.

Using the experimental intensities of the respective bands, I_A, I_B, ..., and I_H, and the Raman scattering activities calculated for the model compounds (Table 1) as I_{xy}, we can evaluate the conformation fractions f_{xy} for the respective bonds of the dodecyl chain in $C_{12}E_5$. However, the experimental data available in this work do not allow determination of all of the conformational fractions uniquely, but give only possible ranges of their values. In this way, we determined the ranges of the trans fractions $f_T(O-C_1)$ and $f_T(C_1-C_2)$ from the spectral data of C_{12}-1-d_1-E_5 and C_{12}-2-d_1-E_5, respectively, and the ranges of the trans fractions $f_T(C_3-C_4-C_5)$, $f_T(C_5-C_6-C_7)$, $f_T(C_7-C_8-C_9)$, and $f_T(C_9-C_{10}-C_{11})$ from the spectral data of C_{12}-4-d_1-E_5, C_{12}-6-d_1-E_5, C_{12}-8-d_1-E_5, and C_{12}-10-d_1-E_5, respectively. The evaluated ranges of the respective f_T values are narrow enough (mostly 0.03) to make their explicit indication in diagrams unnecessary, and the midpoints of the ranges will be used for representing the f_T values. In the present spectral analysis, band D for C_{12}-2-d_1-E_5 was poorly resolved, leading to ill-defined $f_T(C_2-C_3)$ values. Accordingly, we did not adopt these values for our discussion. The values for $f_T(C_1-C_2)$ derived from the spectra of the same monodeuterated species were not affected in substance by this problem.

Conformational Behavior of Surfactant Molecules. Figure 4 shows the temperature dependence of the trans fractions f_T for the respective bonds of the dodecyl chain and the oxyethylene-adjoining O−C bond at different compositions. The trans fractions decrease continuously with increasing temperature without showing their discontinuities at the phase transitions, indicating smooth changes in the trans−gauche conformational equilibria of the C−C bond with temperature. Similar conformational behavior with temperature has been observed for the $C_{12}E_3$−water system, showing no discontinuous change at the L_α/L_2 phase transition.[23]

From the inverse temperature dependence of the logarithm of the ratio of the gauche fraction f_G to the trans fraction f_T for the respective bonds in the L_α phase (75 wt %) of the $C_{12}E_5$−water system, apparent enthalpy differences between the gauche and trans conformations, ΔH ($H_G - H_T$), were evaluated as given in Table 3. The results for the $C_{k-1}-C_k-C_{k+1}$ bonds (k = 4, 6, 8, and 10) indicate that the trans conformation is more stable than the gauche conformation by approximately 4−5 kJ mol^{-1}. The enthalpy difference for the $(O)C_1-C_2(C_3)$ bond is, however, quite small, as the gauche conformation of this bond is stabilized by an attractive intramolecular $C_3H\cdots O$ interaction.[47] The enthalpy difference for the $O-C_1$ bond is larger than that for the C−C bonds. The enthalpy differences for the bonds in the dodecyl chain and the oxyethylene-adjoining O−C bond in the neat liquid have been measured for $C_{12}E_3$,[23] and the results are given in Table 3 for comparison with the present results for the L_α phase. It is interesting to note that the trans conformation is consistently more stabilized in the L_α phase than in the neat liquid, due most probably to the confinement of the alkyl chain in the cylindrical structure in the lamella.

Figure 5 shows the composition dependence of the trans fractions f_T for the dodecyl chain in the $C_{12}E_5$−water system at

TABLE 1: Calculated C−D Bond Lengths (r), Diagonal Force Constants (k), Raman Scattering Activities (A), and Wavenumbers (ν) of C−D Stretching Vibrations, and Observed Wavenumbers (ν_{obsd}) for Model Compounds

skeletal conformation[a]	local conformation[b]	calculated[c] r/Å	k/mdyn Å^{-1}	A/Å^4 amu^{-1}	ν^d/cm^{-1}	ν_{obsd}[e]/cm^{-1}
		$CH_3O-CHD-CH_2CH_2CH_2CH_2CH_3$				
G^+T	CO/tg/CC	1.0936	6.869	46.11	2248.7	2173
G^+G^+	CO/tg/CC	1.0938	6.867	49.40	2248.2	2173
G^-G^-	CO/gt/CC	1.1006	6.459	67.48	2184.3	2128
TG^-	CO/gt/CC	1.1012	6.426	65.05	2178.5	2128
G^-T	CO/gg/CC	1.1014	6.420	35.00	2178.8	2128
TT	CO/gg/CC	1.1021	6.384	40.92	2172.5	2113
TG^+	CO/gg/CC	1.1025	6.364	43.10	2169.1	2113
		$CH_3OCH_2-CHD-CH_2CH_2CH_2CH_3$				
TG^-	OC/gt/CC	1.0948	6.795	57.93	2239.1	2167
G^-G^-	OC/gt/CC	1.0951	6.779	61.85	2235.8	2167
TT	OC/gg/CC	1.0954	6.765	41.06	2234.4	2155
TG^+	OC/gg/CC	1.0957	6.747	44.05	2231.5	2155
G^-T	OC/gg/CC	1.0961	6.735	43.53	2229.4	2155
G^+T	OC/tg/CC	1.0972	6.679	44.49	2220.7	2142
G^+G^+	OC/tg/CC	1.0973	6.677	47.17	2220.2	2142
		$CH_3OCH_2CH_2CH_2-CHD-CH_2CH_3$				
TG^-	CC/gt/CC	1.0966	6.683	46.43	2220.3	2153
G^-G^-	CC/gt/CC	1.0969	6.673	50.72	2218.4	2153
G^+T	CC/tg/CC	1.0970	6.665	56.30	2217.6	2153
G^+G^+	CC/tg/CC	1.0972	6.657	61.38	2216.0	2153
TT	CC/gg/CC	1.0977	6.637	40.63	2213.4	2136
TG^+	CC/gg/CC	1.0979	6.626	43.28	2211.7	2136
G^-T	CC/gg/CC	1.0979	6.625	43.56	2211.5	2136
		$CH_3CH_2CH_2-CHD-CH_2CH_2CH_3$				
TG^-	CC/gt/CC	1.0970	6.657	49.21	2216.5	2153
G^+T	CC/tg/CC	1.0970	6.657	49.21	2216.5	2153
G^+G^+	CC/tg/CC	1.0972	6.654	53.64	2215.8	2153
G^-G^-	CC/gt/CC	1.0972	6.654	53.64	2215.8	2153
TT	CC/gg/CC	1.0978	6.623	39.17	2211.5	2136
TG^+	CC/gg/CC	1.0981	6.608	41.65	2208.6	2136
G^-T	CC/gg/CC	1.0981	6.608	41.65	2208.6	2136

[a] For the conformational forms, see Figure 2. The *R*-configuration is assumed. The conformations shown are only for the bonds that are indicated explicitly by a dash in the chemical formula, and the conformations for all other bonds are trans. [b]For the conformation designation, see text. [c]Calculated at the B3LYP/6-311+G(d,p) level. [d]Unscaled wavenumbers. [e]The observed wavenumbers for $CH_3O-CHD-CH_2CH_2CH_2CH_2CH_3$, $CH_3OCH_2-CHD-CH_2CH_2CH_2CH_3$, and $CH_3OCH_2CH_2CH_2-CHD-CH_2CH_3$ are taken from ref 24, and those for $CH_3CH_2CH_2-CHD-CH_2CH_2CH_3$ are actually the observed wavenumbers for $CH_3CH_2CH_2-CHD-CH_2CH_3$ (hexane-3-d_1) taken from ref 23.

TABLE 2: Observed C−D Stretching Wavenumbers (ν_{obsd}) and Half Widths ($\Delta\nu_{1/2}$) for C_{12}-1-d_1-E_5, C_{12}-2-d_1-E_5, and C_{12}-k-d_1-E_5 (k = 4, 6, 8, and 10) and C−D Stretching Wavenumbers (ν_{obsd}(model)) for Pertinent Model Compounds

band[a]	ν_{obsd}/cm^{-1} ($\Delta\nu_{1/2}$/cm^{-1})	ν_{obsd}(model)/cm^{-1}
	C_{12}-1-d_1-E_5	
A	2183 (60)	2173[b]
B	2140 (60)	2128[b]
C	2116 (66)	2113[b]
	C_{12}-2-d_1-E_5	
D	2178 (50)	2167[b]
E	2158 (37)	2155[b]
F	2145 (37)	2142[b]
	C_{12}-k-d_1-E_5 (k = 4, 6, 8, and 10)	
G	2153 (38)	2153[c]
H	2136 (33)	2136[c]

[a] For the band designation, see Figure 3. [b]Hexyl methyl ether.[24] [c]Hexane.[23]

four temperatures. The trans fractions for the O−C_1, C_1−C_2, and C_{k-1}−C_k−C_{k+1} bonds (k = 4, 6, 8, and 10) do not change significantly with increasing water content. Also, no distinct discontinuities of the changes in conformation are observed at the L_1/L_α and H_1/L_α phase transitions in most cases, although the structures of molecular assemblies in different liquid-crystalline phases differ greatly from one another. The conformational behavior of the C_{k-1}−C_k−C_{k+1} bonds (k = 4, 6, 8, and 10) is essentially the same in the composition region from 40 to 75 wt %. These composition-dependent conformational changes for the $C_{12}E_5$−water system are consistent with those for the $C_{12}E_3$−water system previously studied.[23]

In Figure 6 the trans fractions f_T are plotted as a function of the position on the dodecyl chain at different compositions and temperatures. The trans fraction for the O−C_1 bond is the highest (0.65−0.75), and that for the C_1−C_2 bond is the lowest (0.50−0.55) among the bonds studied. For the C_3−C_4−···−C_{10}−C_{11} bonds, the maximum f_T is observed at C_5−C_6−C_7. These results are consistent with the apparent enthalpy differences given in Table 3, as well as with the previous experimental and theoretical results on simple model compounds;[48,49] the trans conformations of the (C)C−C(C) and (C)O−C(C) bonds are more stable than the gauche conformations by 2.0−4.0 and 4.5−6.0 kJ mol^{-1}, respectively, and the gauche conformation of the (O)C−C(C) bond is more stable than the trans conformation by approximately 0.4 kJ mol^{-1}. It is noted that the profiles of the trans fraction with respect to the positions on the alkyl chain (Figure 6) are similar to one another irrespective of the phases and the compositions. The conformation profiles for the $C_{12}E_5$−water system are again quite similar to those for the $C_{12}E_3$−water system, giving the maximum f_T at C_5−C_6−C_7.[23]

Figure 7 shows the infrared spectra of aqueous solutions of $C_{12}E_5$ at 10 °C for different compositions. The spectra in the

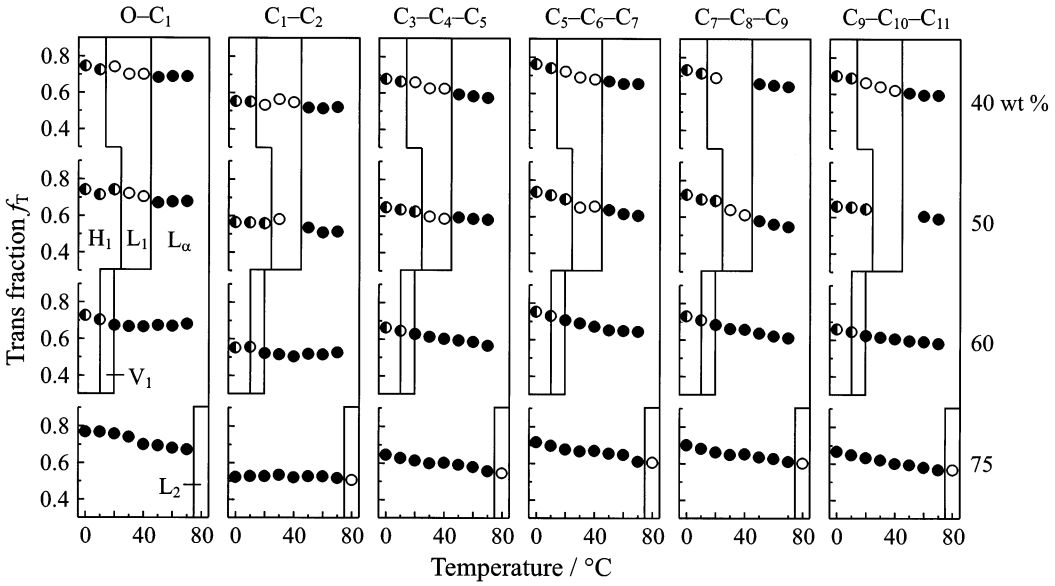

Figure 4. Temperature dependence of the trans fractions f_T for the respective bonds of the dodecyl chain at different compositions. Filled, half-filled, and open symbols are used respectively for the L_α, H_1, and isotropic L_1 or L_2 phases.

TABLE 3: Observed Enthalpy Differences ($H_G - H_T$) between the Gauche and Trans Conformations around Dodecyl C−C Bonds and the Oxyethylene-Adjoining O−C Bond for $C_{12}E_5$−Water (L_α Phase) and $C_{12}E_3$ (Neat Liquid)

	$H_G - H_T$/kJ mol^{-1}	
bond[a]	$C_{12}E_5$−water (L_α phase)[b]	$C_{12}E_3$ (neat liquid)[c]
O−C_1	6.2 ± 0.6	2.5 ± 0.8
C_1−C_2	0.5 ± 0.3	−0.0 ± 0.8
C_3−C_4−C_5	3.8 ± 0.3	3.3 ± 1.7
C_5−C_6−C_7	4.6 ± 0.4	1.7 ± 0.8
C_7−C_8−C_9	4.1 ± 0.3	2.9 ± 0.8
C_9−C_{10}−C_{11}	4.4 ± 0.2	

[a] For the numbering of atoms, see text. [b] Present work. [c] Reference 23.

1300−1400 cm^{-1} region were analyzed to study the conformational behavior of the pentakis(oxyethylene) chain in the $C_{12}E_5$ molecule. In the analysis we used the well-defined conformation key bands at 1330 and 1350 cm^{-1} of poly(oxyethylene) chains;[50] the former is due to the CH_2 wagging mode of the trans conformation around the (O)C−C(O) bond, and the latter is due to the same mode of the gauche conformation. In Figure 7, the ratio of the absorbance of the peak heights for the two bands, A_{1350}/A_{1330}, is plotted against the composition. The plot shows that the absorbance ratio increases with increasing water content, indicating that the gauche conformation of the (O)C−C(O) bond is more favored with more water, in agreement with the previous infrared results on oligo(oxyethylene)s.[51−53]

The preference of the gauche conformation around the (O)C−C(O) bond in oligo(oxyethylene) chains in water has been explained by reason that this conformation is stabilized by the hydrogen bond network of water molecules, wherein the O−CH_2−CH_2−O segments with the gauche conformation around the (O)C−C(O) bond are favorably incorporated.[51,52,54,55] Another factor that stabilizes the gauche conformation is favorable electrostatic interactions between water with high polarity and the gauche O−CH_2−CH_2−O segments with larger dipole moment than the trans.[53] By the reasoning mentioned above, the conformation around the (O)C−C(O) bond in oligo(oxyethylene) chains depends heavily on the water content. This result contrasts with the conformational behavior of the (C)C−C(C) bond of the alkyl chain, which does not show significant conformational changes with water content as mentioned above.

Analysis of Deuterium NMR Spectra in the Liquid-Crystalline Phases. The quadrupole coupling of the deuterium nucleus with the electric field gradient causes splittings of NMR frequencies.[56] For aliphatic C−D bonds, the electric field gradient is axially symmetric with its principal axis along the bond direction. Deuterium NMR spectroscopy can thus be an excellent method for studying molecular orientation.[27−32,57−62] The quadrupole splitting of the two deuterium transitions is given by

$$\Delta\nu = \delta(3\cos^2\theta - 1) \qquad (5)$$

where δ is $^3/_4$ times the quadrupole coupling constant e^2qQ/h with a value of 167 kHz for aliphatic C−D bonds and θ is the angle between the magnetic field and the principal axis of the electric field gradient tensor, that is, the C−D bond direction.[61,62]

In isotropic phases such as L_1, L_2, and V_1, the surfactant molecules experience rapid isotropic motions, resulting in space averaging of $(3\cos^2\theta - 1)$ to effectively zero. Accordingly, only a singlet peak appears in the spectra of these phases. In anisotropic liquid-crystalline phases such as L_α and H_1, on the other hand, the quadrupole splitting is motionally averaged over the C−D bond orientations because of rapid anisotropic molecular motions, for example, interconversions between different conformational states, that take place in a time short compared to the inverse of the quadrupole interaction. The averaged quadrupole splitting for aliphatic C−D bonds in uniaxial liquid-crystalline phases can be rewritten as

$$\langle\Delta\nu\rangle = \delta(3\cos^2\alpha - 1)(1/2)(3\cos^2\beta - 1)S_{CD} \qquad (6)$$

where α is the angle between the phase axis (the normal of the uniaxial phase surface) and the magnetic field, β is the angle between the phase axis and the normal of the hydrophobic/hydrophilic interface, and S_{CD} is a motionally averaged parameter called the order parameter of the C−D bond being given by $(1/2)\langle 3\cos^2\gamma - 1\rangle$ with the angle γ between the normal of the hydrophobic/hydrophilic interface and the C−D bond direction. The order parameter S_{CD} thus is a measure of the motionally averaged orientation of the C−D bond with respect

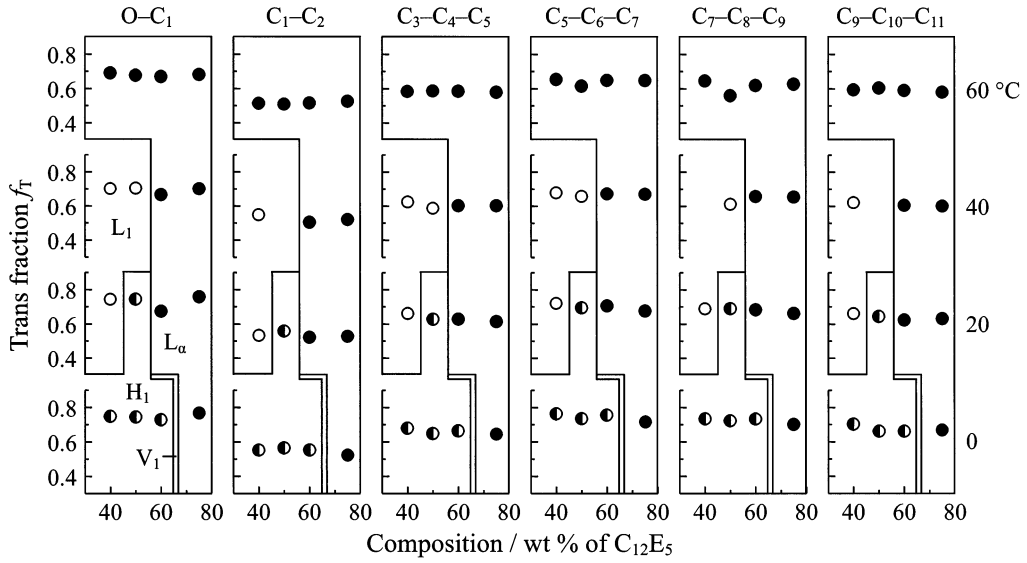

Figure 5. Composition dependence of the trans fractions f_T for the respective bonds of the dodecyl chain at different temperatures. For symbols, see caption for Figure 4.

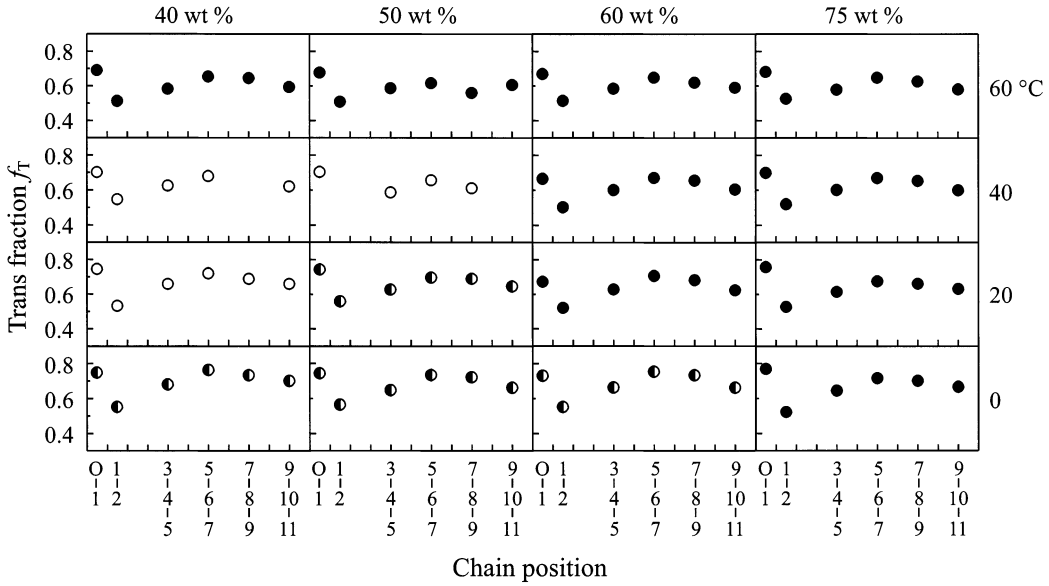

Figure 6. Positional dependence of the trans fractions f_T for the dodecyl chain at different temperatures and compositions. Carbon atoms are indicated by their numbers. For symbols, see caption for Figure 4.

to the normal of the hydrophobic/hydrophilic interface. The conformational conversion from trans to gauche in the molecular chain leads, in general, to a decrease of the order parameter $|S_{CD}|$.[26,58]

The absolute value of the order parameter for the uniaxial liquid-crystalline phases is obtained from the splitting of the maxima, corresponding to $\alpha = 90°$, of the doublet spectra as

$$|S_{CD}| = |\langle \Delta\nu \rangle_{90°}/[\delta(1/2)(3\cos^2\beta - 1)]| \qquad (7)$$

In the L_α phase the phase axis is parallel to the normal of the hydrophobic/hydrophilic interface ($\beta = 0°$), while in the H_1 phase it is perpendicular to the normal of the interface ($\beta = 90°$). Accordingly, for the same value of $|S_{CD}|$, the quadrupole splitting for the H_1 phase is half that for the L_α phase.

Figure 8 shows typical deuterium NMR spectra of aqueous solutions of various alkyl-deuterated and oxyethylene-deuterated species of $C_{12}E_5$. The spectrum of the alkyl-*block*-deuterated species C_{12}-d_{23}-E_5 (Figure 8a) is composed of several quadrupole splittings associated with the deuterium nuclei located at different carbon positions on the dodecyl chain. Use of the selectively alkyl-monodeuterated species, C_{12}-*k*-d_1-E_3 ($k = 1$, 2, 4, 6, 8, and 10) studied previously[30] and C_{12}-*k*-d_1-E_5 ($k = 1$, 2, 4, 6, 8, and 10) (partly shown in Figure 8b−d), makes the assignments of the quadrupole splittings for C_{12}-d_{23}-E_5 unambiguous, as shown in Figure 8a. From the observed splittings for C_{12}-*k*-d_1-E_5 ($k = 1$, 2, 4, 6, 8, and 10) and C_{12}-d_{23}-E_5, the order parameters $|S_{CD}|$ of the C−D bonds at the carbon positions 1, 2, and 4−12 were evaluated using eq 7. When displaying the data of the order parameters in subsequent diagrams, we will omit some of them to avoid complication.

The deuterium NMR spectra of aqueous solutions of the oxyethylene-*block*-deuterated species $C_{12}E_5$-d_{20} in the L_α and H_1 phases are shown in Figure 8e and g, respectively. The observed quadrupole splittings were assigned, as shown in Figure 8e, to the deuterium nuclei at different carbon positions on the pentakis(oxyethylene) chain by utilizing the results obtained for an oxyethylene-*block*-deuterated compound CH_3-$(CH_2)_{11}(OCD_2CD_2)_6OCD_3$.[58] In the spectrum of $C_{12}E_5$-d_{20} in

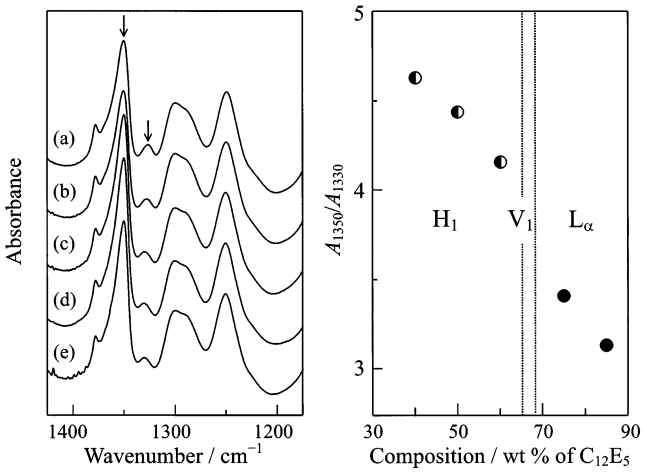

Figure 7. Infrared spectra in the 1175−1425 cm^{-1} region of aqueous solutions of $C_{12}E_5$ at 10 °C for the compositions 85 (a), 75 (b), 60 (c), 50 (d), and 40 wt % $C_{12}E_5$ (e), where arrows indicate the conformation key bands at 1330 and 1350 cm^{-1}, and composition dependence of the absorbance ratio A_{1350}/A_{1330}. For symbols, see caption for Figure 4.

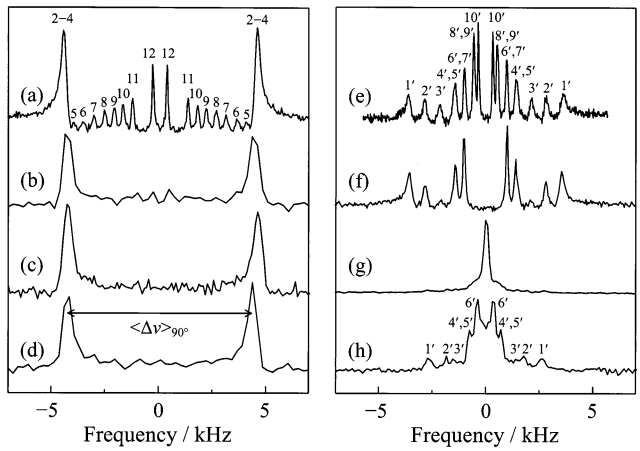

Figure 8. Deuterium NMR spectra of 50 wt % aqueous solutions at 60 °C of C_{12}-d_{23}-E_5 (a), C_{12}-1-d_1-E_5 (b), C_{12}-2-d_1-E_5 (c), C_{12}-4-d_1-E_5 (d), $C_{12}E_5$-d_{20} (e), and $C_{12}E_3$-d_{12}-E_2 (f), and those of 50 wt % aqueous solutions at 0 °C of $C_{12}E_5$-d_{20} (g) and $C_{12}E_3$-d_{12}-E_2 (h). Spectra a−f are of the L_α phase, and spectra g and h are of the H_1 phase. The assignments of the quadrupole splittings to respective deuterium nuclei are given in spectra a, e, and h.

the H_1 phase (Figure 8g), a strong singlet peak is observed along with a number of much weaker doublets. The apparent singlet at the center is actually a superposition of a number of doublets with very small splittings associated with the deuterium nuclei at the carbons near the hydroxyl terminal. The prominent appearance of the center peak makes the identification of the much weaker doublets difficult. To solve this problem, we examined the spectra of the oxyethylene-partially deuterated species $C_{12}E_3$-d_{12}-E_2, for which the hydrogens only at the carbons $C_{1'}$ through $C_{6'}$ are deuterated. The spectrum of this species in the H_1 phase (Figure 8h) in fact clearly shows, when signals are expanded, the doublets associated with the deuterium nuclei at the carbons $C_{1'}$ through $C_{6'}$. From the quadrupole splittings observed for $C_{12}E_3$-d_{12}-E_2 and $C_{12}E_5$-d_{20}, the order parameters $|S_{CD}|$ of the C−D bonds for the pentakis(oxyethylene) chain were evaluated.

Figure 9 shows the NMR spectra of 50 wt % aqueous solutions of C_{12}-2-d_1-E_5, C_{12}-d_{23}-E_5, $C_{12}E_5$-d_{20}, and $C_{12}E_3$-d_{12}-E_2 measured at several temperatures from 0 to 80 °C. On the basis of these spectra and the phase diagram prepared by Mitchel et al.[8] (Figure 1), we can examine the phase transitions of the $C_{12}E_5$−water system along the composition 50 wt % $C_{12}E_5$. Observations of a singlet peak at 80 °C for all species evidence the two-phase region, W + L_2, consisting of two isotropic phases at this temperature. With decreasing temperature from 80 °C, the quadrupole splittings emerge at 75 °C, indicating a phase transition has taken place from W + L_2 to L_α. At 50 °C, the splittings disappear and a singlet peak characteristic of the isotropic structure appears. This observation confirms that the phase transition from L_α to L_1 occurs at this temperature. At 20 °C, the splittings appear again, being consistent with the phase transition from L_1 to H_1. According to the reported phase diagram[8] (Figure 1), the phases on the line 50 wt % at 50 and 20 °C were L_α and L_1, respectively, which are inconsistent with the phases we determined, L_1 and H_1. This inconsistency is associated most probably with a small amount of impurities contained in the sample or with the effect of deuterium substitution on the phase behavior.[63,64]

Order Parameters of the C−D Bonds. The order parameters $|S_{CD}|$ of the C−D bonds at the carbon positions C_1 through C_{10} on the dodecyl chain and the carbon positions $C_{1'}$ through $C_{10'}$ on the pentakis(oxyethylene) chain are shown in Figure 10 as a function of temperature at four compositions. In the L_α phase at 75 wt %, the values of the order parameters for all of the carbon positions on the alkyl chain and for the carbon positions of the first few oxyethylene units from the alkyl/oligo(oxyethylene) interface decrease continuously with increasing temperature. This behavior of the order parameters with varying temperature is consistent with the result that the population of the gauche conformation around the (C)C−C(C) bond increases relative to that of the trans conformation at higher temperatures; the energy difference between these conformations was evaluated as approximately 4 kJ mol^{-1} (Table 3). Figure 10 indicates that the changes of the $|S_{CD}|$ values with temperature for the oligo(oxyethylene) chain are smaller than those for the alkyl chain. This observation for the oligo(oxyethylene) chain is consistent with the infrared and Raman spectroscopic results that the trans−gauche−trans conformation of the (C)O−CH_2−CH_2−O(C) segment is highly stabilized in water by a favorable hydration structure[51−53] and that the population of the gauche conformation around the (O)C−C(O) bond decreases with increasing temperature.[50,65]

A remarkable observation in Figure 10 is that, at the phase transition from H_1 to L_α via isotropic L_1 or V_1, the $|S_{CD}|$ values for all of the carbon positions on the alkyl chain and for the carbon positions of the first few oxyethylene units from the alkyl/oligo(oxyethylene) interface show big discontinuities. This distinctive behavior of the order parameters is not due to conformational interconversions of the alkyl chain, because the trans fractions derived from the Raman measurements do not show discontinuities at the phase transition (Figure 4). Implications of this behavior will be discussed later.

The composition dependence of the order parameters of $C_{12}E_5$ at several temperatures is shown in Figure 11. With increasing surfactant content, the $|S_{CD}|$ values increase continuously within each of the H_1 and L_α phases, but they show discontinuous changes at the phase transition from H_1 to L_α. These discontinuities are in accord with the corresponding discontinuities observed when temperature is varied.

Figure 12 shows the $|S_{CD}|$ values for the H_1 and L_α phases as a function of the position of the carbon atom on the molecular chain. The order parameters of the dodecyl chain vary smoothly along the molecular chain, exhibiting a maximum at carbons C_4 to C_2. This behavior of the order parameters for the $C_{12}E_5$−

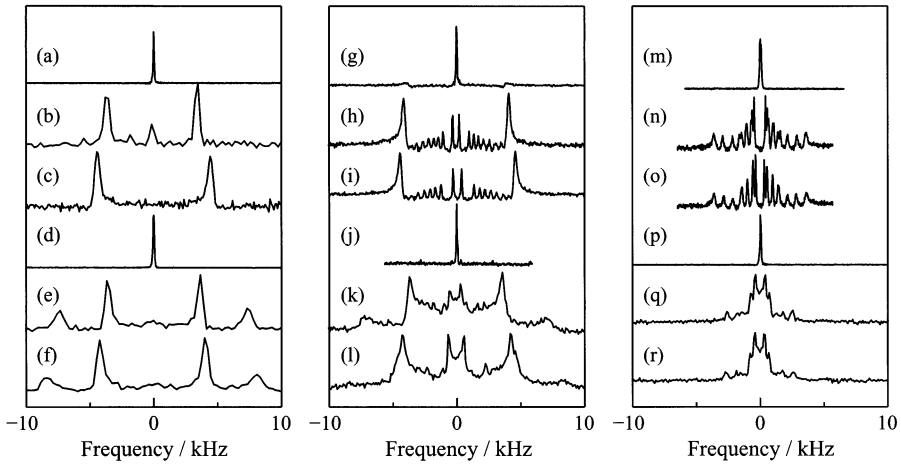

Figure 9. Deuterium NMR spectra of 50 wt % aqueous solutions of C_{12}-2-d_1-E_5 (a−f), C_{12}-d_{23}-E_5 (g−l), $C_{12}E_5$-d_{20} (m−p), and $C_{12}E_3$-d_{12}-E_2 (q, r) at the temperatures 80 (a, g, m; W + L_2 two-phase region), 75 (b, h, n; L_α phase), 60 (c, i, o; L_α phase), 50 (d, j, p; L_1 phase), 20 (e, k, q; H_1 phase), and 0 °C (f, l, r; H_1 phase).

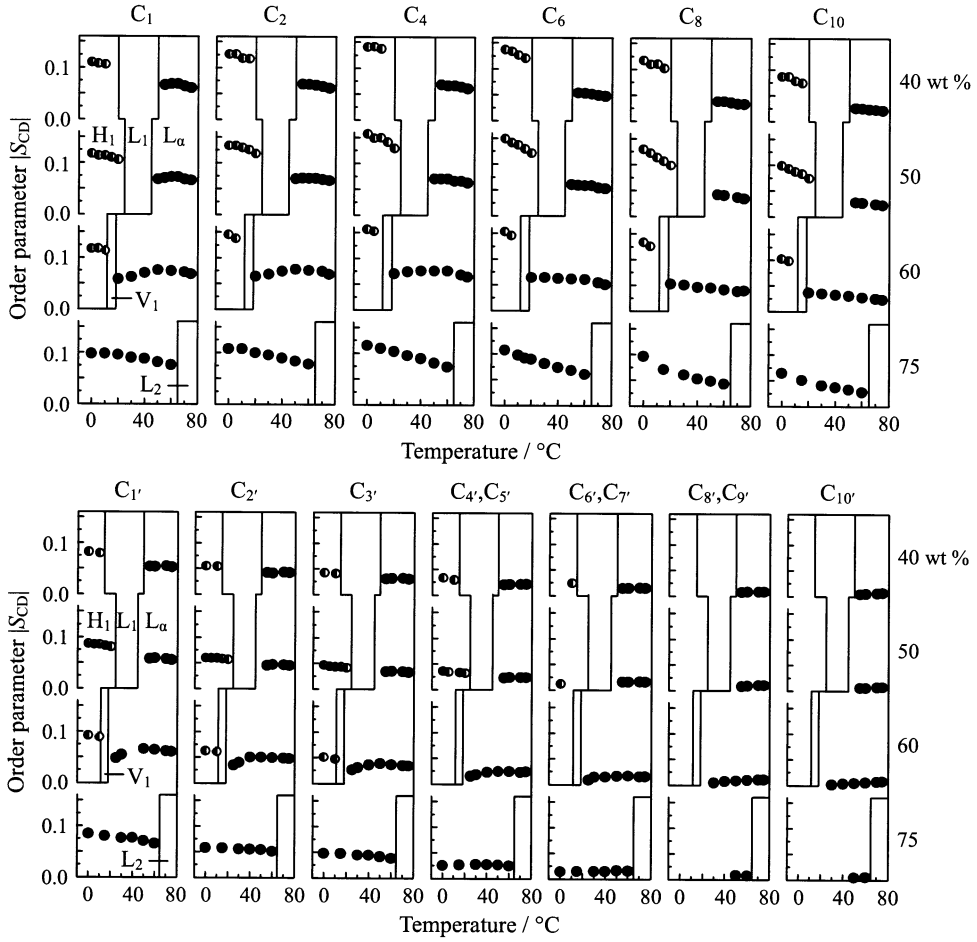

Figure 10. Temperature dependence of the order parameters $|S_{CD}|$ for the respective carbon positions on the dodecyl and pentakis(oxyethylene) chains at different compositions. For symbols, see caption for Figure 4.

water system is similar to that for the $C_{12}E_3$−water system studied in our previous work.[30] The order profiles of the nonionic surfactants $C_{12}E_5$ and $C_{12}E_3$ differ from those of ionic surfactants such as potassium and sodium palmitates, whose order parameters show their largest values at the first carbon position next to the polar headgroup and decrease monotonically along the chain toward the methyl terminal.[61,62] For oligo(oxyethylene) nonionic surfactants, the stability of the trans conformation around the (O)C_1−C_2(C_3) bond next to the oligo(oxyethylene) chain is lowered, as the counterpart gauche conformation is stabilized by an attractive intramolecular $C_3H\cdots O$ interaction.[47] This specific conformational property of the (O)C_1−C_2(C_3) bond results in the decrease of the order parameters at the first few carbon atoms of the alkyl chain near the alkyl/oligo(oxyethylene) interface. It is noted in Figure 12 that the $|S_{CD}|$ values of the oligo(oxyethylene) chain decrease stepwise as the position of the relevant carbon atom approaches the hydroxyl terminal. These stepwise changes of the order parameters can be explained by the involvement of conformationally unlike segments, (O)CH_2−CH_2(O) and (C)CH_2−O−

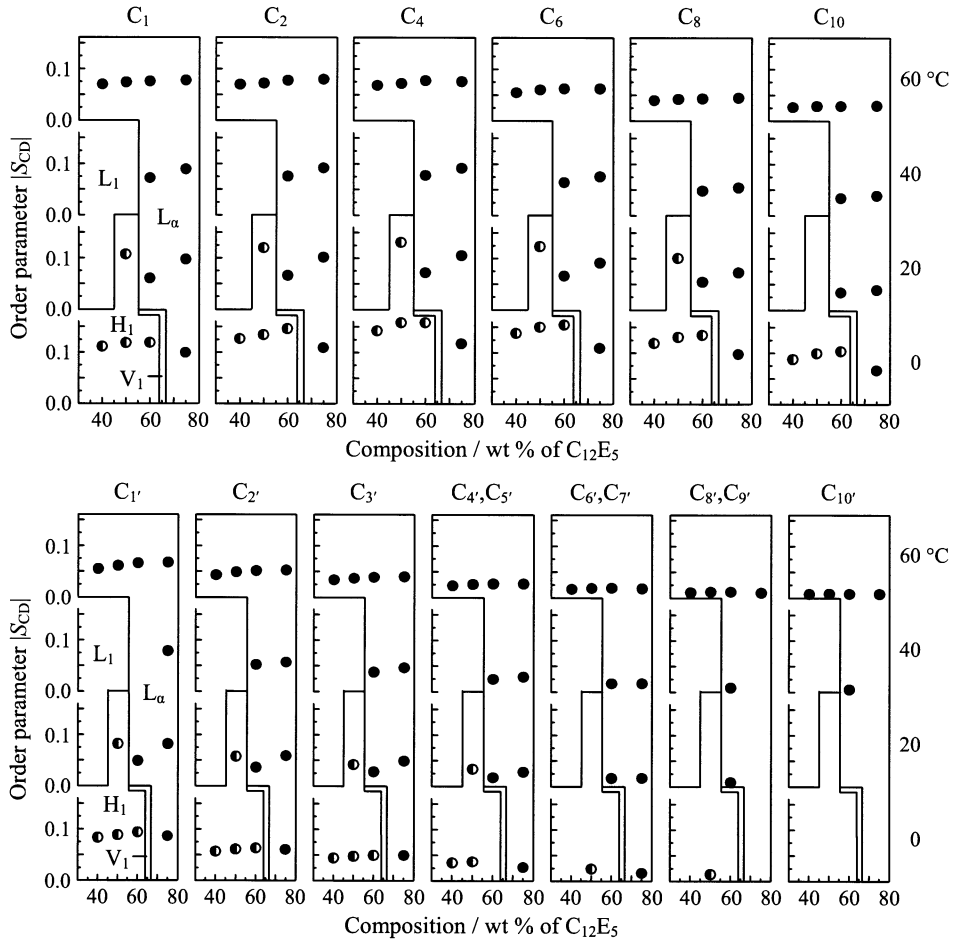

Figure 11. Composition dependence of the order parameters $|S_{CD}|$ for the respective carbon positions on the dodecyl and pentakis(oxyethylene) chains at different temperatures. For symbols, see caption for Figure 4.

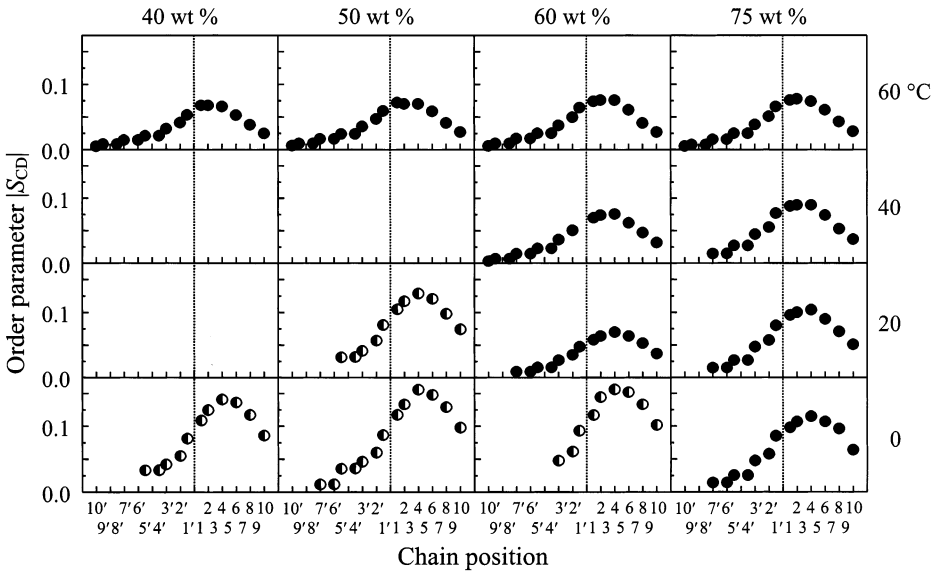

Figure 12. Positional dependence of the order parameters $|S_{CD}|$ for the respective carbon positions on the dodecyl and pentakis(oxyethylene) chains at different temperatures and compositions. For symbols, see caption for Figure 4.

CH_2(C), in the chain; namely, the former prefers the gauche conformation, while the latter prefers the trans−trans conformation.

Comparison of the Results from Raman and Deuterium NMR Spectroscopies. The Raman results show that the conformation of the dodecyl chain in the $C_{12}E_5$−water system changes continuously with increasing temperature across the different phases (Figure 4). The deuterium NMR results show, on the other hand, that, with increasing temperature, the order parameters exhibit distinct discontinuities at the phase transition from H_1 to L_α via isotropic L_1 or V_1 (Figure 10). The apparent difference between the Raman and NMR results is interpreted as follows. The phenomena of molecular motions observed by NMR spectroscopy with its time scale 10^{-5} to 10^{-4} s are

different from those observed by Raman spectroscopy with its time scale 10^{-14} to 10^{-13} s. Conformational changes of molecules take place in the time scale 10^{-11} to 10^{-10} s.[29] Thus, the trans fraction f_T is a statistical average of the local conformations of individual conformers, and the order parameter $|S_{CD}|$ is a motional average of the orientation of the C−D bond with respect to the normal of the hydrophobic/hydrophilic interface. This implies that NMR spectroscopy provides us with information of more macroscopic phenomena than vibrational spectroscopy. The order parameter depends not only on conformational changes but also on chain reorientation motions, for example, rotation around the long axis and restricted wobbling motion of a whole molecule within the aggregate, with an effective correlation time of 10^{-9} to 10^{-7} s.[27,60]

According to Petersen and Chan,[27] the order parameter $|S_{CD}|$ can be divided into two contributions $|S_{chain}|$ and $|S_{con}|$; the chain order $|S_{chain}|$ describes the angular deflection of the molecular chain axis with respect to the normal of the hydrophobic/hydrophilic interface, and the conformational order $|S_{con}|$ describes the orientation of the C−D bond with respect to the instantaneous molecular chain axis. The chain order $|S_{chain}|$ is expected to decrease in regions near the phase transition, because the chain reorientation is likely to be enhanced with increasing fluctuation of the hydrophobic/hydrophilic interface, as suggested by the unfavorable value of the packing parameter[5,66] to be discussed later. The continuous conformational changes of the $C_{12}E_5$ molecules with varying temperature imply that the conformational order $|S_{con}|$ also changes continuously without discontinuities at the phase transition. Accordingly, the observed discontinuities of the $|S_{CD}|$ values at the phase transition can be ascribed to the change of the chain order $|S_{chain}|$, which is caused by wobbling motions of the whole surfactant molecule.[27−29,32,59] Thus, the observed changes of the order parameters $|S_{CD}|$ (Figures 10 and 11) are explained by taking account of the two contributions, $|S_{chain}|$ and $|S_{con}|$.

Figure 12 indicates that, at 0 and 20 °C, the $|S_{CD}|$ values of the dodecyl chain in the H_1 phase are larger than the values in the L_α phase. The Raman results in Figure 6 show, on the other hand, that the trans fraction profiles of the dodecyl chain in the H_1 and L_α phases are similar to each other. The increase of the $|S_{CD}|$ values in the H_1 phase is attributed for the most part to the lowering of the wobbling motion of the whole alkyl chain, since the space allowed for the methyl terminal to move in the H_1 phase is smaller than that in the L_α phase. According to Figure 12, the maximum value of the order parameter $|S_{CD}|$ is observed at C_4 at 0 and 20 °C for both L_α and H_1 phases, but it shifts to C_2 at a higher temperature, 60 °C. On the other hand, no shifts of the maximum value with temperature are observed for the trans fraction f_T of the alkyl chain (Figure 6). It is expected that, when temperature is increased, the effect of van der Waals forces between the alkyl chains reduces more rapidly than the effect of the hydrogen-bonding forces between the oligo(oxyethylene) chain and water. The shift of the maximum value of $|S_{CD}|$ is thus a consequence of the different rates of reduction in the effects of the two relevant forces associated with the molecular motion.

Implications of Molecular Structure and Motions in Phase Behavior. Nonionic surfactant molecules C_nE_m assemble to form supramolecular structures in the liquid-crystalline phases by attractive intermolecular interactions such as van der Waals interaction and hydrogen bonding, and the total energy of the relevant intermolecular interactions well exceeds the kinetic energy.[5] Taking account of the closely packed hydrophobic alkyl chains with the van der Waals contact, we can elucidate our experimental results in terms of the packing parameter, v/a_0l_c,[5,66] where v is the volume of the hydrophobic alkyl chain, l_c is the critical chain length, namely the maximum effective length that the chains can assume, and a_0 is the optimal surface area per molecule at the alkyl/water interface, namely an effective cross-sectional area of the hydrophobic/hydrophilic interface per surfactant molecule. The most favorable value of the packing parameter is around $^1/_3$ to $^1/_2$ for the H_1 phase and is around 1 for the L_α phase.[5]

Our previous Raman spectroscopic study on the $C_{12}E_5$−water and $C_{12}E_6$−water systems[43] has shown that, when water between the hydrophilic surfaces of the lamellae is removed, rapid destruction of the tetrahedral hydrogen bond network occurs, leading to a phase transition from L_α to L_2. With decreasing water content, the population of the gauche conformation around the (O)C−C(O) bond of oligo(oxyethylene) chains in the L_α phase decreases,[43] in agreement with the present observation (Figure 7). These experimental findings show that the well-defined hydrogen bond network, in which the oligo(oxyethylene) chains with their (O)C−C(O) bonds in the gauche conformation are favorably incorporated, interconnects the lamellae with their hydrophilic surfaces facing to each other. This implies that the interlamellar water plays an important role in keeping the L_α phase stabilized.

We will discuss below the structural behavior of the $C_{12}E_5$−water system with increasing water content. In the region of high surfactant content at low temperatures, addition of water promotes the formation of a hydrogen bond network between the lamellae and thereby promotes the conformational changes from trans to gauche around the (O)C−C(O) bonds. According to the molecular dynamics simulations,[55] oligo(oxyethylene) chains in water assume a helical structure with the gauche conformation around the (O)C−C(O) bonds. This structure is well defined and has a sizable expansion. Applying this expanded structure to the oligo(oxyethylene) chains of the $C_{12}E_5$ molecules in water gives an increased surface area per molecule at the alkyl/water interface, a_0, with increasing water content. Accordingly, the value of the packing parameter decreases, resulting, in fact, in the consecutive phase transitions from L_α to V_1, H_1, and L_1 at temperatures lower than approximately 20 °C (Figure 1). As described before, the big discontinuities of the order parameters at the phase transition between L_α and H_1 (Figure 11) are elucidated by the enhanced wobbling motion of the whole surfactant molecule near the phase boundary, where the packing parameter should have values unfavorable for the respective phase structures.

With increasing temperature, on the other hand, the hydrogen bond network destructs due to the thermodynamically unfavorable restructuring of water molecules at higher temperatures, as has actually been observed by Raman spectroscopy.[67] This results in a decrease of a_0, accompanied by a conformational change from gauche to trans around the (O)C−C(O) bond, and leads to a decrease of the mean curvature of the alkyl/oligo(oxyethylene) interface.[68] Thus, when temperature is increased, the mean curvature of the interface in the H_1 phase decreases progressively toward zero, allowing the void available for the hydrophobic chains to undergo the conformational changes and wobbling motions, as manifested by the significant decreases of the trans fractions and the order parameters (Figures 4 and 10). The decreased mean curvature eventually results in the phase transition from H_1 to L_α via V_1 at compositions around 60 wt % (Figure 1).

The mechanisms of the phase transitions for the C_nE_m−water systems have been discussed previously.[8] The H_1/V_1 and $V_1/$

L_α phase transitions observed when the composition is varied at constant temperature or when the temperature is varied at constant composition were characterized as "shape transitions", which occur because of the unfavorable curvature being balanced by intermicellar repulsions or because of the constraints on the value of a_0.[8] Our interpretation of the experimental results from this and previous studies is fully consistent with the mechanism of the shape transitions.

The L_α phase of the $C_{12}E_5$−water system extends over a large area from approximately 30 to 75 wt % $C_{12}E_5$ at temperatures around 60 °C (Figure 1). Throughout this composition range, the trans fractions of the dodecyl chain and the order parameters of the dodecyl and pentakis(oxyethylene) chains are almost constant (Figures 5 and 11). These observations indicate that the water added to the L_α phase does not affect the structure and motions of the surfactant molecules but rather participates in the formation of the interlamellar water region. This consequence ensures our interpretation that the presence of interlamellar water is important for stabilizing the L_α phase. Our results of the stability of the L_α phase are consistent with the previous results from small-angle X-ray scattering of the L_α phase of the $C_{12}E_3$−water and $C_{12}E_4$−water systems;[69] namely, the effective cross-sectional area of a surfactant molecule and the half thickness of the hydrophobic layer are almost constant irrespective of water content in the system, while the interlamellar spacing is extended by swelling with water.

Conclusions

A combined C−D stretching Raman and deuterium NMR spectroscopic method was applied to a study of the molecular and phase structure of the $C_{12}E_5$−water system. The Raman results showed that the trans fractions of the C−C bonds of the dodecyl chain decrease continuously with increasing temperature across the different phases. The NMR results showed, on the other hand, that, with increasing temperature, the order parameters exhibit distinct discontinuities at the phase transition from H_1 to L_α via isotropic L_1 or V_1. The results from the two spectroscopic methods reflect the difference in their time scale, 10^{-5} to 10^{-4} s for NMR and 10^{-14} to 10^{-13} s for Raman spectroscopy. The behavior of the order parameters was explained by taking account of two factors, the chain order (angular deflection of the molecular chain axis with respect to the normal of the hydrophobic/hydrophilic interface) and the conformational order (orientation of the C−D bond with respect to the instantaneous molecular chain axis). The observed discontinuities of the order parameters at the phase transition can be ascribed to the change of the chain order, which is caused by wobbling motions of the whole surfactant molecule. The temperature-dependent shift of the position on the alkyl chain, at which the order parameters show their maximum, is explained by the different rates of reduction, with increasing temperature, of van der Waals forces between the alkyl chains and hydrogen-bonding forces between the oligo(oxyethylene) chain and water. The stability of the L_α phase is maintained by the presence of interlamellar water. A combination of Raman and NMR spectroscopies with their different time scales has provided complementary information on the structure of molecules in the liquid-crystalline phases.

Acknowledgment. This work was partially supported by Grant-in-Aid for Scientific Research No. 10440176 from the Ministry of Education, Culture, Sports, Science, and Technology of Japan.

References and Notes

(1) Tanford, C. *The Hydrophobic Effect: Formation of Micelles and Biological Membranes*, 2nd ed.; Wiley: New York, 1980.
(2) Degiorgio, V., Corti, M., Eds. *Physics of Amphiphiles: Micelles, Vesicles and Microemulsions*; North-Holland: Amsterdam, 1985.
(3) Tiddy, G. J. T. In *Modern Trends of Colloid Science in Chemistry and Biology*; Eicke, H.-F., Ed.; Birkhäuser: Basel, 1985; pp 148−183.
(4) Ben-Shaul, A.; Gelbart, W. M. *Annu. Rev. Phys. Chem.* **1985**, *36*, 179−211.
(5) Israelachvili, J. N. *Intermolecular and Surface Forces*, 2nd ed.; Academic Press: London, 1992.
(6) Laughlin, R. G. *The Aqueous Phase Behavior of Surfactants*; Academic Press: London, 1994.
(7) Jönsson, B.; Lindman, B.; Holmberg, R.; Kronberg, B. *Surfactants and Polymers in Aqueous Solution*; Wiley: Chichester, U.K., 1998.
(8) Mitchel, D. J.; Tiddy, G. J. T.; Warning, L.; Bostock, T.; McDonald, M. P. *J. Chem. Soc., Faraday Trans. 1* **1983**, *79*, 975−1000.
(9) Leaver, M. S.; Olsson, U.; Wennerström, H.; Strey, R.; Würz, U. *J. Chem. Soc., Faraday Trans.* **1995**, *91*, 4269−4274.
(10) Kunieda, H.; Ozawa, K.; Huang, K.-L. *J. Phys. Chem. B* **1998**, *102*, 831−838.
(11) The term "frequency" has been customarily used in the field of vibrational spectroscopy to indicate the quantity actually given in units of cm^{-1} rather than Hz. We use, in this paper, the appropriate terminology of "wavenumber" for this quantity, following SI usage recommended by IUPAC.[12]
(12) Mills, I.; Cvitaš, T.; Homann, K.; Kallay, N.; Kuchitsu, K. *Quantities, Units and Symbols in Physical Chemistry*; IUPAC, Blackwell: Oxford, 1988.
(13) Painter, P. C.; Coleman, M. M.; Koenig, J. L. *The Theory of Vibrational Spectroscopy and Its Application to Polymeric Materials*; Wiley: New York, 1982.
(14) Scheuing, D. R., Ed. *Fourier Transform Infrared Spectroscopy in Colloid and Interface Science*; American Chemical Society: Washington, DC, 1990.
(15) Gaber, B. P.; Yager, P.; Peticolas, W. L. *Biophys. J.* **1978**, *21*, 161−176.
(16) Gaber, B. P.; Yager, P.; Peticolas, W. L. *Biophys. J.* **1978**, *22*, 191−207.
(17) Gaber, B. P.; Yager, P.; Peticolas, W. L. *Biophys. J.* **1978**, *24*, 677−688.
(18) Yager, P.; Peticolas, W. L. *Biophys. J.* **1980**, *31*, 359−370.
(19) Yager, P.; Peticolas, W. L. *Biochim. Biophys. Acta* **1982**, *688*, 775−785.
(20) Ohno, K.; Takagi, Y.; Matsuura, H. *J. Phys. Chem.* **1993**, *97*, 5530−5534.
(21) Ohno, K.; Yoshida, H.; Matsuura, H. *Spectrochim. Acta, Part A* **1996**, *52*, 1377−1389.
(22) Masatoki, S.; Ohno, K.; Yoshida, H.; Matsuura, H. *Chem. Lett.* **1996**, 149−150.
(23) Masatoki, S.; Ohno, K.; Yoshida, H.; Matsuura, H. *J. Phys. Chem.* **1996**, *100*, 8487−8498.
(24) Ohno, K.; Abe, H.; Masatoki, S.; Yoshida, H.; Matsuura, H. *J. Phys. Chem.* **1996**, *100*, 12674−12679.
(25) Matsuura, H. *Prog. Colloid Polym. Sci.* **1997**, *106*, 42−48.
(26) Seelig, J. *Q. Rev. Biophys.* **1977**, *10*, 353−418.
(27) Petersen, N. O.; Chan, S. I. *Biochemistry* **1977**, *16*, 2657−2667.
(28) Tuchtenhagen, J.; Ziegler, W.; Blume, A. *Eur. Biophys. J.* **1994**, *23*, 323−335.
(29) Ziegler, W.; Blume, A. *Spectrochim. Acta, Part A* **1995**, *51*, 1763−1778.
(30) Tonegawa, A.; Ohno, K.; Matsuura, H.; Yamada, K.; Okuda, T. *Chem. Lett.* **2000**, 324−325.
(31) Tonegawa, A.; Michiue, A.; Ohno, K.; Matsuura, H.; Yamada, K.; Okuda, T. *Chem. Lett.* **2001**, 818−819.
(32) Tonegawa, A.; Michiue, A.; Masuda, T.; Ohno, K.; Matsuura, H.; Yamada, K.; Okuda, T. *Z. Naturforsch. A* **2002**, *57*, 320−326.
(33) Levitt, M. H. *Spin Dynamics: Basics of Nuclear Magnetic Resonance*, 1st ed.; Wiley: Chichester, UK, 2001; pp 184−188 and 477−511.
(34) Sekera, V. C.; Marvel, C. S. *J. Am. Chem. Soc.* **1933**, *55*, 345−349.
(35) Kharasch, M. S.; McNab, M. C.; Mayo, F. R. *J. Am. Chem. Soc.* **1933**, *55*, 2531−2533.
(36) Friedman, L.; Shani, A. *J. Am. Chem. Soc.* **1974**, *96*, 7101−7103.
(37) Hsiao, C. Y. Y.; Ottaway, C. A.; Wetlaufer, D. B. *Lipids* **1974**, *9*, 913−915.
(38) Zimmermann, H. *Liq. Cryst.* **1989**, *4*, 591−618.
(39) Frisch, M. J.; Trucks, G. W.; Schlegel, H. B.; Scuseria, G. E.; Robb, M. A.; Cheeseman, J. R.; Zakrzewski, V. G.; Montgomery, J. A., Jr.; Stratmann, R. E.; Burant, J. C.; Dapprich, S.; Millam, J. M.; Daniels, A. D.; Kudin, K. N.; Strain, M. C.; Farkas, O.; Tomasi, J.; Barone, V.; Cossi,

M.; Cammi, R.; Mennucci, B.; Pomelli, C.; Adamo, C.; Clifford, S.; Ochterski, J.; Petersson, G. A.; Ayala, P. Y.; Cui, Q.; Morokuma, K.; Malick, D. K.; Rabuck, A. D.; Raghavachari, K.; Foresman, J. B.; Cioslowski, J.; Ortiz, J. V.; Stefanov, B. B.; Liu, G.; Liashenko, A.; Piskorz, P.; Komaromi, I.; Gomperts, R.; Martin, R. L.; Fox, D. J.; Keith, T.; Al-Laham, M. A.; Peng, C. Y.; Nanayakkara, A.; Gonzalez, C.; Challacombe, M.; Gill, P. M. W.; Johnson, B.; Chen, W.; Wong, M. W.; Andres, J. L.; Gonzalez, C.; Head-Gordon, M.; Replogle, E. S.; Pople, J. A. *GAUSSIAN 98*, revision A.5; Gaussian, Inc.: Pittsburgh, PA, 1998.

(40) Becke, A. D. *J. Chem. Phys.* **1993**, *98*, 5648−5652.

(41) Lee, C.; Yang, W.; Parr, R. G. *Phys. Rev. B* **1988**, *37*, 785−789.

(42) Gaufrès, R.; Bribes, J.-L.; Sportouch, S.; Ammour, J.; Maillols, J. *J. Raman Spectrosc.* **1988**, *19*, 149−153.

(43) Marinov, V. S.; Nickolov, Z. S.; Matsuura, H. *J. Phys. Chem. B* **2001**, *105*, 9953−9959.

(44) Ghosh, H. N.; Sapre, A. V.; RamaRao, K. V. S. *Chem. Phys. Lett.* **1996**, *255*, 49−57.

(45) To test the validity of the model compounds, hexyl methyl ether and heptane, we performed density functional calculations at the B3LYP/6-311+G(d,p) level on intermediate compounds between the two adopted model compounds and $C_{12}E_5$, namely C_8E_1 and dodecane. The calculated wavenumbers of the C−D stretching vibrations for C_8E_1 in the all-trans conformation are 2177.8 (C_8E_1-1-d_1), 2233.4 (-2-d_1), 2213.8 (-4-d_1), 2211.3 (-5-d_1), 2210.6 (-6-d_1), and 2218.0 cm^{-1} (-7-d_1), the first three of which are compared with the wavenumbers for the model compound hexyl methyl ether in the all-trans conformation, 2172.5 (hexyl-1-d_1 methyl ether), 2234.4 (-2-d_1), and 2213.4 cm^{-1}(-4-d_1) (Table 1). The calculated wavenumbers of the C−D stretching vibrations for dodecane are 2218.2 (dodecane-2-d_1), 2210.2 (-3-d_1), 2211.0 (-4-d_1), 2211.2 (-5-d_1), and 2211.1 cm^{-1} (-6-d_1), showing that the wavenumbers for those except dodecane-2-d_1 (C−D stretching at the carbon atom next to the methyl terminal) are essentially equal to one another and to the wavenumber for the model compound heptane-4-d_1, 2211.5 cm^{-1} (Table 1). These results indicate that the compounds hexyl methyl ether and heptane can be adequate models for $C_{12}E_5$.

(46) Flory, P. J. *Statistical Mechanics of Chain Molecules*; Hanser: Munich, FRG, 1989.

(47) Ohno, K.; Yoshida, H.; Watanabe, H.; Fujita, T.; Matsuura, H. *J. Phys. Chem.* **1994**, *98*, 6924−6930.

(48) Kitagawa, T.; Kusaki, K.; Miyazawa, T. *Bull. Chem. Soc. Jpn.* **1973**, *46*, 3685−3687.

(49) Wiberg, K. B.; Murcko, M. A. *J. Am. Chem. Soc.* **1988**, *110*, 8029−8038.

(50) Matsuura, H.; Fukuhara, K. *J. Polym. Sci., Part B: Polym. Phys.* **1986**, *24*, 1383−1400.

(51) Matsuura, H.; Fukuhara, K. *J. Mol. Struct.* **1985**, *126*, 251−260.

(52) Begum, R.; Matsuura, H. *J. Chem. Soc., Faraday Trans.* **1997**, *93*, 3839−3848.

(53) Wahab, S. A.; Matsuura, H. *Phys. Chem. Chem. Phys.* **2001**, *3*, 4689−4695.

(54) Depner, M.; Schürmann, B. L.; Auriemma, F. *Mol. Phys.* **1991**, *74*, 715−733.

(55) Tasaki, K. *J. Am. Chem. Soc.* **1996**, *118*, 8459−8468.

(56) Abragam, A. *The Principles of Nuclear Magnetism*; Clarendon: Oxford, 1961.

(57) Seelig, J.; Niederberger, W. *J. Am. Chem. Soc.* **1974**, *96*, 2069−2072.

(58) Schnepp, W.; Schmidt, C. *Ber. Bunsen-Ges. Phys. Chem.* **1993**, *97*, 1399−1402.

(59) Schnepp, W.; Disch, S.; Schmidt, C. *Liq. Cryst.* **1993**, *14*, 843−852.

(60) Firouzi, A.; Schaefer, D. J.; Tolbert, S. H.; Stucky, G. D.; Chmelka, B. F. *J. Am. Chem. Soc.* **1997**, *119*, 9466−9477.

(61) Davis, J. H.; Jeffrey, K. R. *Chem. Phys. Lipids* **1977**, *20*, 87−104.

(62) Abdolall, K.; Burnell, E. E.; Valic, M. I. *Chem. Phys. Lipids* **1977**, *20*, 115−129.

(63) Guard-Friar, D.; Chen, C. H.; Engle, A. S. *J. Phys. Chem.* **1985**, *89*, 1810−1813.

(64) Caboi, F.; Monduzzi, M. *Langmuir* **1996**, *12*, 3548−3556.

(65) Wahab, S. A.; Matsuura, H. *J. Mol. Struct.* **2002**, *606*, 35−43.

(66) Israelachvili, J. N.; Mitchell, D. J.; Ninham, B. W. *J. Chem. Soc., Faraday Trans.* **1976**, *72*, 1525−1568.

(67) Marinov, V. S.; Matsuura, H. *J. Mol. Struct.* **2002**, *610*, 105−112.

(68) Rendall, K.; Tiddy, G. J. T. *J. Chem. Soc., Faraday Trans. 1* **1984**, *80*, 3339−3357.

(69) Huang, K.-L.; Shigeta, K.; Kunieda, H. *Prog. Colloid Polym. Sci.* **1998**, *110*, 171−174.